

Study of Fatigue Damage in Shot Peened Aluminium Alloys using Acoustic Emission and Macro/Microscopic X-Ray Diffraction Investigations

J.P. Bonnafé, G. Maeder, Ecole Nationale Supérieure d'Arts et Métiers, Paris;
C. Bathias, Université de Technologie de Compiègne, Compiègne, France.

ABSTRACT

Aeronautic industry needs to use materials which combine lightness and high mechanical characteristics, under static solicitations as well as under dynamic ones. In this last case, the study of fatigue behaviour of the material becomes very important. High strength aluminium alloys such as 2024 and 7054 are a good choice and for that are usually used in such cases. Moreover, these alloys are often shot peened to improve their fatigue strength.

The recording of acoustic emission allows to detect the three stages of damage growth: plastic deformation of the surface, microcracks formation and macrocracking. The experiment pointed to the conclusion that the damage leading to crack initiation occurs in the following manner: cyclic cold working of the surface together with a rapid evolution of residual stresses, stabilisation of these stresses and a plastic deformation of the surface layers, appearance of the first microcracks without any change in the residual stresses and then, the ascendancy of one or two macrocracks together with complete relaxation of the macrostresses in the close neighbourhood of this macrocrack.

INTRODUCTION

We call fatigue of materials the general properties modifications during cycles which can lead to failure. The materials behaviours studies during fatigue, which are often carried out at macroscopic scale, either by S-N curves (1), either by solicitation modes studies (1), either by cyclic cold working studies (2), must be completed at microscopic scale by crack initiation and crack propagation studies (3), (4) taking into account the initiation potential sites, their number and their types (5). The use of fracture mechanic concepts allows, besides, to determine the maximum size of admissible cracks (6) and to study crack propagation velocity as a function of parameters such as R ratio and grains size (7).

In addition to these numerous parameters which operate upon materials behaviour, we must add residual stresses influence. These residual stresses, which are the result of elaboration process and various thermal and mechanical treatments, play an important role at macroscopic scale as well as at microscopic one, and at the surface as well as under the surface. Different studies give us an idea of what can be expected for stress distributions in subsurface layers, for milling (8), (9) and more often for shot peening (10), (11), (12), (13), (14).

Concerning the residual stress influence upon fatigue behaviour of materials, these residual stresses are superposed to service stresses so that allowable stress can be increased or decreased; this superposition is only valid for elastic behaviour. At macroscopic scale, Mattson and al. (15) have shown the linear relation between residual stress at the surface and endurance limit. Syren and al. (16) introduced an hardness factor to link bending fatigue strength to residual stress (always by a linear relation), when Starker and al. (17) show the influence of the initial distribution in the subsurface layers. At microscopic scale, Evans and al. (18) separate the effect of macrostress and microstrain in relation with hardness. Goto (19) was more precise by giving a linear relation between endurance limit and the X-ray diffraction peak width.

Concerning evolutions of residual stress during fatigue, it is generally admitted that the stability of residual stresses depends on the hardness of the material. Starker and al. (20), comparing two different states of the same steel, or Schutz (21), comparing steel and aluminium alloy, show that harder the material is more stable the residual stresses are. Apart residual stresses, two parameters are usually taken into account in fatigue studies, which are applied stress and R ratio (minimum applied stress/maximum applied stress). Recent studies in this way (22), (23), (24) show that with these two parameters, we can get relaxation or no relaxation of residual stresses, and even an increase of residual stresses. Compressive residual stresses induced by shot peening tend to show the same behaviour: relaxation at the first cycles, and then stabilisation until the end. At last, studies about evolutions of microstrains, mainly Japanese studies (25), (26), show that hardness also influence strain at this scale and that we can separate materials into "annealed" materials and "cold worked" materials, according to their fatigue behaviour.

USED TECHNOLOGY

The study of acoustic emission linked to plastic deformation is a non destructive testing method which, through the use of an elastic wave, reveals the harmfulness of what exists in the material. The signal obtained, at first approximation, can be defined as the superposition of a continuous signal associated to dislocation movements and a discrete signal linked to macroscopic and microscopic ruptures (fracture of precipitates, microcracking, propagation of cracks, etc.). The curve of the cumulative counting as a function of the number of cycles, represented in bilogarithmic coordinates, allows to distinct three phases of damage of the material (27). Zone I is a non damaging zone, zone II is a microscopic damage zone (initiation and propagation of microcracks) and zone III is a macroscopic damage zone (initiation and propagation of macroracks) leading to rupture (figure 1). These three zones are systematically found whatever the initial preparation of the material is: only their limits change (28).

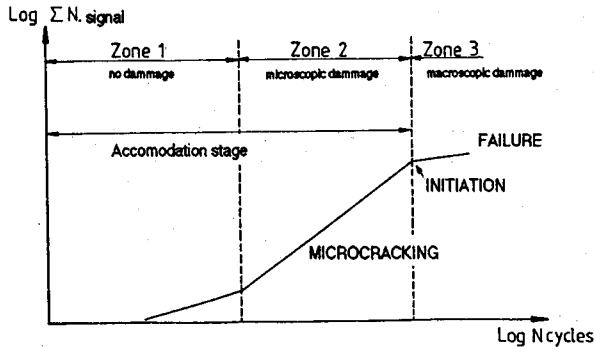


Figure 1 - Acoustic emission definition

Stress measurement by X-ray diffraction is a non destructive method using the property of X-rays to be diffracted by the crystalline structure of materials. The use of this method (29), (30) leads to macroscopic stress by transforming the variations of $d(hkl)$ into a shift in the position of the diffraction peak (using Bragg's law). It also allows to determine microstrains by studying the diffraction peak shape. Indeed, plastic deformation of the material induced cracking in the coherent fields and an increase of their elastic deformation, due to dislocations growth and pile default. This give a widening of diffraction peak. This study can be lead in a qualitative way by measuring the peak width at middle height, or in a quantitative way, using Stokes's method and Warren's models of peak shape (31).

EXPERIMENTAL PROCEDURE

Materials studied in this work are two high strength aluminium alloys, 2024 alloy (AU4G1 - AlCuMg2) and 7075 alloy (AZ5GU - AlZnMgCu1,5). These two alloys are studied in T351 state for 2024 alloy and in T7351 state for 7075 alloy, and their mechanical characteristics are given in the table on figure 2.

		Long.	Trans.
2024	R _{0,2} (MPa)	405	350
	R (MPa)	515	485
	A%	13,5	15,0
7075	R _{0,2} (MPa)	415	415
	R (MPa)	500	495
	A%	12,0	10,5

E=72000 MPa
ν=0,34

Figure 2 - Mechanical characteristics of 2024 and 7075 alloys

For the fatigue tests, chosen samples are unnotched parallelepipeds (160 mm x 50 mm x 20 mm) taken from rolled sheet. We have to notice that the greatest dimension of the sample is in the long transverse direction of rolling. For each material, one single face of sample has been prepared in order to get different states of stress in surface: shot peening (compressive residual

stresses), milling (tensile residual stresses) and electrolytic polishing (nearly no residual stress) as a reference state.

The first stage has been the characterisation of initial geometrical stages (surface roughness) and mechanical states (hardness and residual stresses) for different samples. Residual stress has been determined by mean of X-ray diffraction method, at and under the surface, at macroscopic and microscopic scale. Diffraction conditions have been chosen as follows: K α Cr radiation ($\lambda = 2.2897 \text{ \AA}$, 222 planes, $2\theta = 156.67^\circ$) with an affected depth of about 30 μm and a K1 factor of - 98.5. Every stress has been measured in the longitudinal direction of the bars, where residual stress is parallel to applied stress during fatigue.

The second stage was to determine the different damage zone limits by recording the acoustic emission during a three point bending fatigue test, lead with a R ratio equal to 0.1. Two fatigue fields have been studied, low cycle fatigue and high cycle fatigue. Low cycle fatigue tests were lead under a 500 MPa applied stress, with 10 Hz in frequency. For high cycle fatigue tests, frequency was still 10 Hz but applied stresses have been chosen for an optimal number of cycles at the failure for shot peened samples, around 1.E5 to 2.E5 cycles. It gives an applied stress equal to 440 MPa for 2024 alloy and an applied stress equal to 340 MPa for 7075 alloy.

The following stage has consisted in interrupted fatigue tests in each of the previously determined zones. In order to get more precision about the stress relaxation during the first few cycles, points at 1, 5, 10 and 20 cycles have been added in every result curves.

RESULTS

The results of roughness measurements are as follows:

	Shot peening	Milling	Polishing	
2024	2.81	0.98	0.04	
7075	7.63	0.99	0.05	Ra in μm

The difference in roughness values for shot peened specimens comes from a difference in shot peening process: 2024 alloy is glass peened (FO.15A, $\phi = 0.25 \text{ mm}$) and 7075 is shot peened with iron shots (FO.20A, $\phi = 0.60 \text{ mm}$).

The results of the initial state of stresses measurements are shown on figure 3. They show the following points.

At macroscopic scale:

- shot peening gives compressive residual stresses at the surface (- 300 MPa for 2024 alloy, - 150 MPa for 7075 alloy) with a maximum below the surface. It can also be seen that the shot peened affected depth is varying with the nature of the shots and the material: about 300 μm for glass peened 2024 alloy and 400 μm for shot peened 7075 alloy.
- the milling studied leads to tensile residual stresses on the surface and affects a very thin layer of the material: both milling give almost similar results (+ 50 to + 70 MPa at the surface).

At microscopic scale:

- it can be seen that we can mark the difference between shot peening and milling: for a base metal state characterised by a peak width of $1.8^{\circ}.2\theta$, cold working due to milling is characterised by a peak width of $2.25^{\circ}.2\theta$ (increase equal to 25 %) and cold working due to shot peening is characterised by a peak width of $3.7^{\circ}.2\theta$ (increase equal to 106 %). We can also mark the difference between the two millings and between the two shot peenings, not by the surface value but by the affected depth: 70 μm for milled 7075 alloy, 100 μm for milled 2024 alloy, 250 μm for shot peened 2024 alloy and 400 μm for shot peened 7075 alloy. These values are similar to the ones found at macroscopic scale.

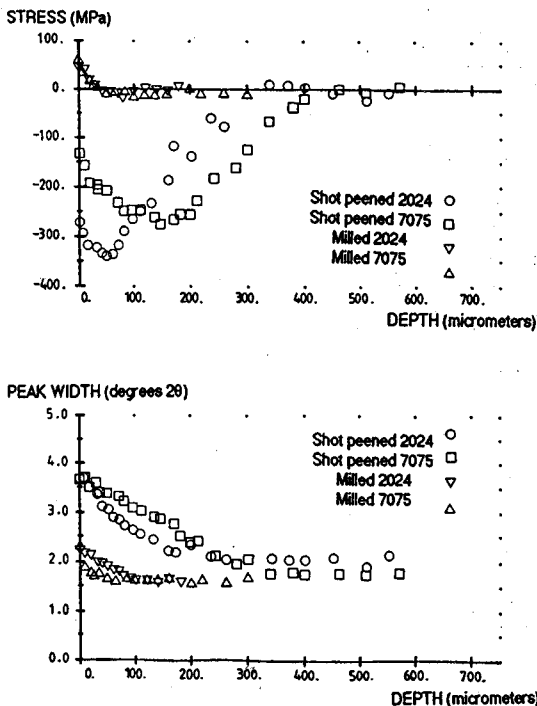


Figure 3 - Initial states of macrostresses and microstrains

The fatigue tests with recording of acoustic emission have given the results shown on the three following figures. The first figure (figure 4) shows the results in the case of the 2024 alloy as an example of cumulative counting versus number of cycles. The second figure (figure 5) is a table in which numeric results about the limits of the damage zones are given for both 2024 and 7075 alloys. These tests have confirmed the interest of shot peening on fatigue life but they mainly show that shot peening with glass beads on 2024 alloy is more effective than shot peening with steel shots on 7075 alloy. Indeed, for the glass peened 2024 alloy, the limits of damage zones are clearly shifted toward larger number of cycles, sign of a delay in the beginning of phenomena. In the case of shot peened 7075 alloy, the delay is less

important. On the other hand, residual stresses from milling and polishing are not different enough to give large variations in the limits of damage zones. A last remark can be done about the results of acoustic emission. When they are presented as apple-pie charts (figure 6), we can notice that except variations due to uncertainty, every chart is identical: we can get the conclusion that whatever the material or the surface preparation may be, the relative durations of damage zones remain the same, even in the case of shot peened materials.

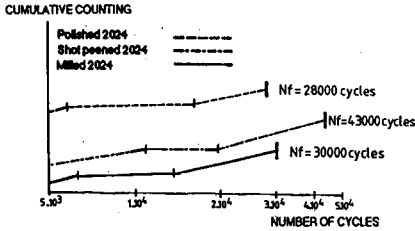
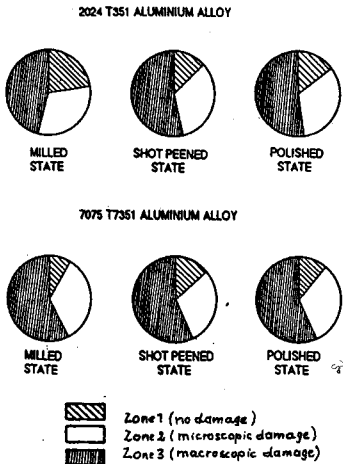


Figure 4 - Damage zones recorded by acoustic emission



LOW CYCLE FATIGUE			
7075	Milled	zone 1	0 to 8910
		zone 2	10120 to 13300
		zone 3	15000 to 20000
	Shot Peened	zone 1	0 to 5000
		zone 2	7300 to 12000
		zone 3	15100 to 24000
Polished	zone 1	0 to 5000	
	zone 2	6300 to 10200	
	zone 3	11700 to 19000	
2024	Milled	zone 1	0 to 4500
		zone 2	5800 to 13500
		zone 3	17400 to 30000
	Shot Peened	zone 1	0 to 10200
		zone 2	11000 to 19500
		zone 3	22900 to 43000
	Polished	zone 1	0 to 4300
		zone 2	5600 to 14100
		zone 3	16200 to 28000
HIGH CYCLE FATIGUE			
7075	Shot Peened	zone 1	0 to 14600
		zone 2	17100 to 118000
		zone 3	121000 to 150000
2024	Shot Peened	zone 1	0 to 14200
		zone 2	16500 to 54100
		zone 3	55900 to 101000

Figure 5 - Damage zones limits

Figure 6 - Relative duration of damage zones

About interrupted fatigue tests, at first, only the surface residual stresses have been measured for all cases. The results are shown on figure 7 for macrostresses and on figure 8 for microstrains characterised by peak widths. At macroscopic level, in low cycle fatigue, we can see that in all cases except polishing where the initial residual stress is zero, there is an important relaxation which happens at the very beginning of the cycling (the points at 20 cycles, and even those at 5 cycles when they exist, show the relaxation is finished yet). On the contrary, in the case of high cycle fatigue (shot peened specimens), this relaxation is less important and seems

to go on (no stabilisation). At microscopic scale, the three surface preparations have different behaviours: we can notice an "hardening" of milled state (cold working and dislocation density increase during fatigue), a "softening" of shot peened state (cold working and dislocation density decrease during fatigue) and an intermediate polished state nearly without "hardening" or "softening".

Milling : $\sigma_{11} = \blacktriangle, \sigma_{22} = \triangle$. Polishing : $\sigma_{11} = \blacklozenge, \sigma_{22} = \lozenge$. Shot peening (L.C.F.) : $\sigma_{11} = \bullet, \sigma_{22} = \circ$
Shot peening (H.C.F.) : $\sigma_{11} = \blacksquare, \sigma_{22} = \square$

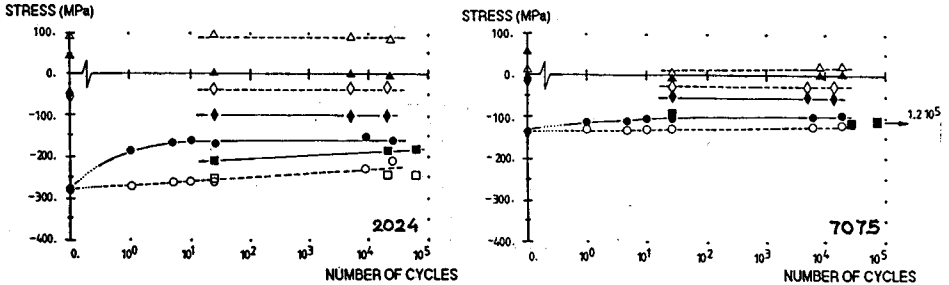


Figure 7 - Surface macrostress variations

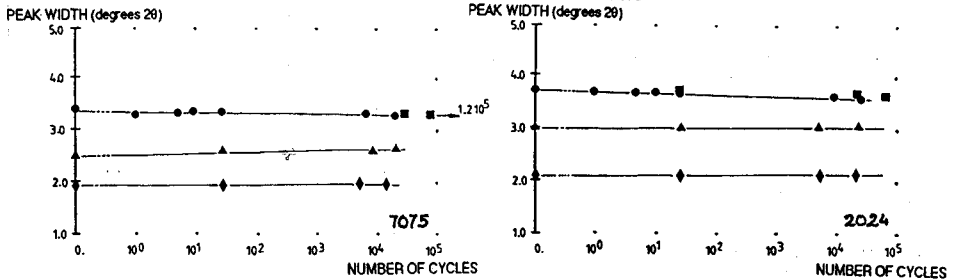


Figure 8 - Surface microstrain variations

These results have been completed, in the case of shot peening, by measurements in depth of the material. We are obliged there to separate low cycle fatigue and high cycle fatigue. At macroscopic scale for low cycle fatigue, we can see on figure 9 that stresses in subsurface layers show the same behaviour than surface stresses, i.e. relaxation in the first few cycles and then stabilisation. On the contrary, in high cycle fatigue cases at macroscopic scale, the relaxation of subsurface stresses is delayed and is happening during all the fatigue test (figure 10). At microscopic scale, peak width variations during low cycle fatigue in the shot peened layers show a "softening" behaviour for the two materials (points during fatigue are under the curve of the initial state points) (figure 11). On the contrary, peak width variations during high cycle fatigue in shot peened layers show a "softening" behaviour for 2024 alloy and an "hardening" behaviour for 7075 alloy (figure 12). Nevertheless, we have to notice that these "softening" and "hardening" behaviours are behaviours of a thin layer of shot peened materials.

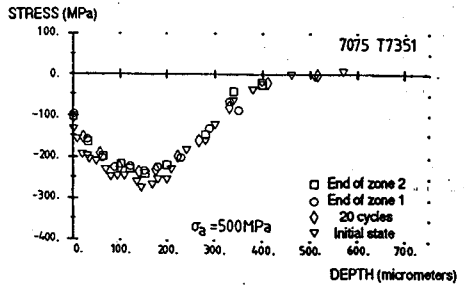
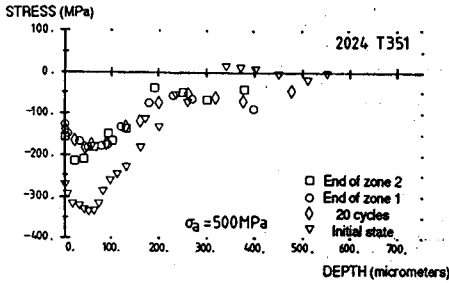


Figure 9 - Macrostress variations in subsurface layers
Case of low cycle fatigue

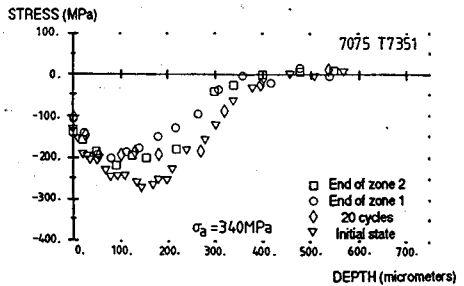
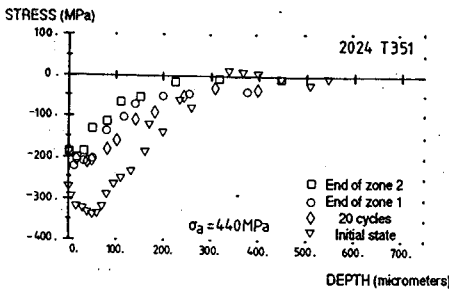


Figure 10 - Macrostress variations in subsurface layers
Case of high cycle fatigue

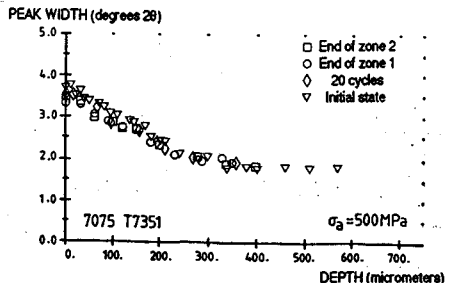
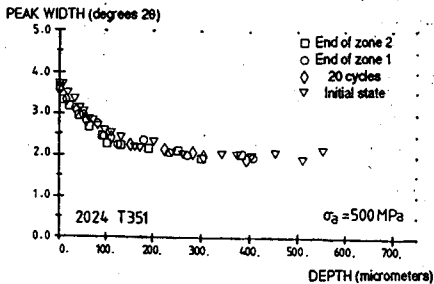


Figure 11 - Microstrain variations in subsurface layers
Case of low cycle fatigue

In a last time, we wanted to do again these measurements using Stokes's method and Warren's model for peak treatment. For milled alloy, and moreover for shot peened alloy, the initial deformation given by the process will hide deformations created by fatigue process. The study of the size of coherent arrays only allows to distinguish cold worked materials from the other ones: 21.7 nm mean valeur for shot peened 2024 alloy, 21.4 nm mean value for the same configuration in high cycle fatigue test, 22.2 nm mean value for milled 2024 alloy and 51.5 nm mean value for polished 2024 alloy.

This result seems to be correct because cold working, which is shown by an increase of dislocation density, reduce the array between two dislocation creation process be.

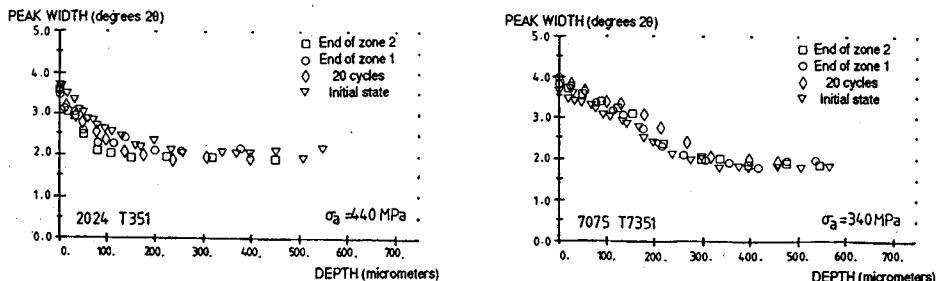


Figure 12 - Microstrain variations in subsurface layers
Case of high cycle fatigue

DISCUSSION

Apart some problems due to grain size in the subsurface layers of shot peened materials and at the surface for other ones, the use of X-ray diffraction for stress measurements can be done without any troubles. The use of a large diffraction spot (\varnothing 4 mm or even 4 mm x 10 mm) allows us, for a great part of measurements, to get away from local discontinuities. However, stress study on cracks boundaries by mean of this technique needs more precautions and longer measurement times. On an other hand, penetration depth of $K\alpha$ chromium radiation in aluminium alloys (30 μ m mean value) allows to get free from surface roughness effects, what is interesting in the case of shot peening.

Fatigue tests with recording of the acoustic emission show that this measurement technique was rather reproductive (zone limits are defined with a mean precision of ± 1000 cycles, it means a relative error of 7 % in the most unfavourable case), and usefull to detect the limits in time for some damaging phenomenon. The use of this method is linked to the minimum size definition of detectable default, which greatly depends on recording conditions and on electronic detection threshold. Experiments carried out by other detection techniques such as electric detection method or optical observation method, allows to precise the validity of acoustic emission method and to fix the macrocracks detection threshold to about 100 μ m.

The results of this study bring some complements in the observation of fatigue behaviour of aluminium alloys. It is confirmed that shot peening brings a profit in life time of parts submitted to fatigue (+ 20 % for 7075 alloy, + 30 % for 2024 alloy). But it has also been shown that this benefit depends on shot peening conditions and that there could exist an optimum treatment. The idea of efficiency of shot peening has been pointed out by the determination of the damage phases: in a "good" shot peening, all the limits of zones are clearly shifted toward a higher number of cycles (for example, in 2024 alloy case, + 50 % at the end of zone I, + 40 % at the end of zone II and at last + 30 % at the failure).

This benefit and this efficiency of shot peening can be explained by a lot of remarks about residual stresses and surface roughness. In the case of glass peened 2024 alloy, surface stress value is higher, as well as maximum stress value under the surface, and this maximum stress is closer to the surface. Moreover, its surface state is better and crack initiation sites are less numerous. At last, we can notice that the relative durations of damage zones stay at constant values whatever the material or its preparation be: zone I last on about 15 to 25 % of total time of failure, zone II last on about 35 to 45 % and the rest is for zone III.

Concerning variations of residual macrostresses during fatigue tests, the results are in complete agreement with the previous published studies. The use of the records of acoustic emission has allowed the determination of the three stages in the evolution of surface residual stresses:

- a quick relaxation of the stresses, more or less important as a function of the initial residual stress and of applied stress. A 500 MPa applied stress causes a 40 % fall in the 2024 residual stress and a 25 % fall in the 7075 residual stress, for low cycle fatigue. For high cycle fatigue, a 440 MPa applied stress causes a 30 % fall in the 2024 residual stress and a 340 MPa applied stress causes a 10 % fall in the 7075 residual stress.
- a stabilisation lasting until the initiation of the first macrocracks (microcracks initiation and propagation are not visible for X-rays),
- a continuation of this stabilisation except in the close neighbourhood of cracks where there is a complexe relaxation of macrostresses.

It must be however specified that in this last phase, the evolutions are not well known particularly because of the X-ray diffraction conditions. The drop of residual stress can happen in a very short time before failure or be limited in a very tiny zone, unaccessible with present experimental techniques. Thus, measurements have been done on broken specimen and they show that at one millimeter from the failure, residual stresses reach 40 MPa and we can imagine a higher tensile strength near the crack tips at the very last cycle.

The previous mentioned steps at the surface are also found in depth for shot peened specimen, in low cycle fatigue tests. We must note that the way back to zero is different for 2024 and 7075 alloys: in case of 2024 alloy, we can see a plateau in subsurface layers. This can be partially explained by the difference between yield stress values and by the difference between $\sigma_a - \sigma_{ys}$ values, as we can observe on the next figure (figure 13). On this figure, σ_e shows the flow limit value. At first cycle, this value is equal to monotonous yield stress, but little by little, it will reach cyclic yield stress. For 7075 alloy, we shall get $\sigma_{cys} < \sigma_e < \sigma_{mys}$ (in fact, measurements during low cycle fatigue tests show that the results are rather $\sigma_{cys} \# \sigma_e \# \sigma_{mys}$). On the contrary, for 2024 alloy, the same tests show that cyclic yield stress raise to a 420 MPa value, it means 20 % more than monotonous yield stress. In this case, we get $\sigma_{mys} < \sigma_e < \sigma_{cys}$.

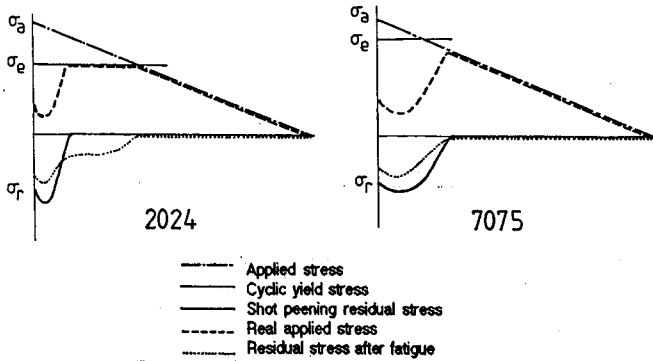


Figure 13 - Stress superposition

At last, it is very likely that, as the maximum value of compressive residual stress under the surface and as this maximum position in depth, roughness given by glass peening compared with the one given by shot peening allows to explain a part of the longer life of 2024 alloy. For example, we can think that if we could improve surface roughness of shot peened 7075 alloy by mean of polishing or by mean of a second shot peening with glass beads without any change in stress repartition or stress value, we could get an increase of life time of specimen. We can see on next figure (figure 14) that his process is fully possible and can keep all favourable effects of shot peened residual stresses. This point is confirmed by results obtained from mechanical polished specimen. As it can be seen on next figure (figure 15), a very good surface state associated to surface residual stresses which are in light compression gives a better life time than one of shot peened specimen. The following step of this study, work in process in this time, will consist to make comparisons possible between the two alloys, by conducting tests on shot peened 24 alloys with steel shots and on glass peened 7075 alloy. The first results shown on are encouraging ones.

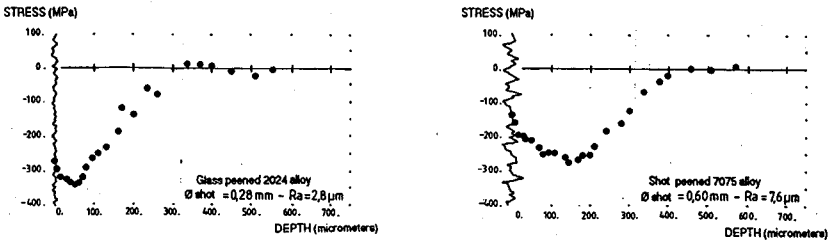


Figure 14 - Shot peening induced roughness

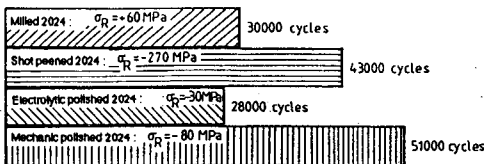


Figure 15 - Influence of surface roughness

CONCLUSION

The study of low cycle fatigue behaviours of materials, although not representative of numerous real cases, presents many advantages. The test times are short, the phenomena are shorter and their interpretations can be more or less easily transposed to high cycle fatigue studies. The use of acoustic emission allows to link the evolutions of residual stresses to a concrete damage phenomenon. Although there is a need of additional results, the study has shown very well the different stages of the evolution of residual stresses in a fatigue sollicitation.

REFERENCES

- (1) RABBE P., 1980, "Mecanismes et mecanique de la fatigue", in La fatigue des materiaux et des structures, C.Bathias, J.P.Bailon, Les Presses de l'Universite de Montreal, Maloines S.A. Editeur, pp 1-29.
- (2) PINEAU A., PETREQUIN P., 1980, "La fatigue plastique oligocyclique", pp 107-161, ib idem (1).
- (3) RABBE P., 1980, "L'amorçage des fissures de fatigue", pp 71-105, ib idem (1).
- (4) COTTRELL A.H., HULL D., 1957, Proc. R. Soc., A242, p 211.
- (5) SIGLER D., MONTPETIT M.C., HAWORTH W.L., 1983, "Metallography of fatigue crack initiation in an overaged high strength aluminium alloy", Metallurgical Transactions A, Volume 14A, may, pp 931-938.
- (6) SCARLIN R.B., STUCHELI A., 1983, "The behaviour of fatigue cracks in shot peened components", Conference on Application of Fracture Mechanics to Materials and Structures, June 20-24th, Fribourg, Germany.
- (7) ZURER A.K., JAMES M.R., MORRIS W.L., 1983, "The effect of grain size on fatigue growth of short cracks", Metallurgical Transactions A, Volume 14A, August, pp 1697-1705.
- (8) SYREN B., WOHLFAHRT H., MACHERAUCH E., 1976, "The influence of residual stresses and surface topography on bending fatigue strength of machined Ck45 in different heat treatment conditions", Proceedings of the 2nd International Conference on Mechanical Behaviour of Materials, Boston, pp 212-235.
- (9) WAKABAYASHI M., MAKAYAMA M., TAMAMURA K., 1982, "Study on residual stresses in unidirectional machined layers", Journal of Japan Society for Precision Engineering, Volume 44, n.6.
- (10) FLAVENOT J.F., NIKU-LARI A., 1976, "Le grenailage de precontrainte", Note Technique n.15 du CETIM.
- (11) CASTEX L., JOUBERT F., 1981, "La determination des precontraintes de grenailage par diffractometrie X et leur modelisation", First International Conference on Shot Peening, ICSP-1, Paris, Pergamon Press Editor, pp 255-262.
- (12) WOHLFAHRT H., 1982, "Shot peening and residual stresses", in Residual Stress and Stress Relaxation, E.Kula, V.Weiss, Plenum Press Editor, p 71.
- (13) GUECHICHI H., CASTEX L., FRELAT J., INGLEBERT G., 1985, "Prevision des contraintes residuelles dues au grenailage", Compte rendu de la 5eme Journee Nationale sur le Grenailage de Precontraintes, CETIM Senlis, 27 novembre, pp 29-45.
- (14) MAEDER G., LEBRUN J.L., DIAMENT A., 1981, "Caracterisation par diffraction X d'une couche grenaillee", pp 263-269, ib idem (11).
- (15) MATTSONS R.L., ROBERTS J.G., 1956, "The effect of residual stresses induced by strain peening upon fatigue strength", Proceedings of the Symposium on Internal Stresses and Fatigue of Metals, Detroit, G.M.Rassweiler and W.L.Grube Editors, pp 337-360.
- (16) ib. idem (8).

- (17) STARKER P., WOHLFAHRT H., MACHERAUCH E., 1979, "Subsurface crack initiation during fatigue as a result of residual stresses", *Fatigue of Engineering Materials and Structures*, Volume 1, pp 319-327.
- (18) EVANS W.P., RICKLEFS R.E., MILLAN J.L., 1965, "X-ray and fatigue studies of hardened and cold worked steels", *Proceedings of the Symposium on Local Atomic Arrangement studied by X-ray diffraction*, Chicago, J.B.Cohen, J.E.Hilliard Editors, Chapter 11.
- (19) GOTO T., 1976, "Application of X-ray stress measurement to pre-service inspection and in-service inspection", pp 1614-1618, *ib idem* (8).
- (20) STARKER P., WOHLFAHRT H., MACHERAUCH E., 1981, "Biegenwechselfestigkeit und Grosseneffekt bei unterschiedlich warmbehandelten strahlproben aus Ck45 nach Kugelstrahlen", pp 613-623, *ib idem* (11).
- (21) SCHUTZ W., 1981, "Fatigue life improvement of high strength materials by shot peening", pp 423-433, *ib idem* (11).
- (22) HIRSH T., VOHRINGER O., MACHERAUCH E., 1984, "Bending fatigue behaviour of differently heat treated and shot peened AlCu5Mg2", *Second International Conference on Shot Peening, ICSP2*, Chicago, H.O.Fuchs Editor, pp 90-101.
- (23) BERGSTROM J., ERICSSON T., 1984, "Relaxation of shot peening induced compressive stress during fatigue of notch steel samples", pp 241-248, *ib idem* (22).
- (24) JAMES M.R., MORRIS W.R., 1983, "Fatigue induced changes in surface residual stress", *Scripta Metallurgica*, Volume 17, pp 1101-1104.
- (25) TAIRA S., 1974, "X-ray examination during fatigue", *Metal Science*, n.8, pp 234-238.
- (26) TAKECHI H., NAMBA K., KUJIWARA K., KAWASAKI K., 1981, "Evaluation of subsurface fatigue damage in strip mill rolls by X-ray diffraction method", *Transactions of the Iron and Steel Institute of Japan*, Volume 21, n.2, pp 92-99.
- (27) HOUSSENI-EMAN M., 1981, "Etude de l'emission acoustique associee a la deformation plastique des metaux sous sollicitations cycliques sous l'action de l'environnement. Applications sur les alliages d'aluminium 2618 AT651 et 2024 T351", *These de Docteur Ingenieur, U.T.C., 26 mars*.
- (28) BONNAFE J.P., 1986, "Etude par diffractometrie X et emission acoustique de l'endommagement par fatigue des alliages d'aluminium a haute resistance grenailles", *These de Doctorat, U.T.C., 16 mai*.
- (29) MAEDER G., LEBRUN J.L., SPRAUEL J.L., 1981, "Present possibilities for the X-ray diffraction method of stress measurement" *NDT International*, October, pp 235-247.
- (30) CASTEX L., 1985, "Evolutions recentes de l'analyse des contraintes par diffractometrie X", *Compte rendu des Journees d'Extensometrie*, Lyon.
- (31) WARREN B.E., 1969, "X-ray diffraction", Addison Wesley Editor.